Evaluation of LS-DYNA® Material Models for the Analysis of Sidewall Curl in Advanced High Strength Steels

Ali Aryanpour [*], Daniel E. Green

Department of Mechanical, Automotive and Materials Engineering,
University of Windsor, 401 Sunset Ave., Windsor, N9B 3P4, ON, Canada

Abstract

Accurate modelling of the Bauschinger effect and anisotropic plasticity in advanced high strength steels (AHSS) is essential in order to accurately predict sidewall curl. In this study, the performance of several constitutive models from the LS-DYNA library was evaluated for the prediction of sidewall curl in a plane-strain channel draw process for two grades of AHSS (TRIP780 and DP980). Since the profile of the channel section after springback results from the recovery of elastic strains in a plastically deformed sheet metal, the stress distributions in the channel section after the forming stage were carefully examined. Deformation modes in the sheet metal included sliding under the binder pressure, successive bending-unbending through a drawbead and drawing over the die entry radius. Material types 24, 36, 37 and 125 were used with shell element formulation 16 in order to select the most accurate combination for predicting sidewall curl. An investigation of simulation results showed that MAT125 predicted the sidewall curvature more accurately than the other models.

Keywords: Sidewall Curl, AHSS, Springback, Yoshida-Uemori

Introduction

Stamping structural rail shaped parts results in two types of springback: section opening and sidewall curl. The section opening springback has long been recognized and compensated by methods such as over bending and crowning. Sidewall curl, however, is still a detrimental factor when forming rail or channel sections (Fig.1) that require tight tolerance of mating surfaces and can cause assembly and welding difficulties. The advanced high strength steels (AHSS) exhibit even more sidewall curl compared to conventional high strength steels (HSS) because of the difference in their strain hardening behaviours. Sidewall curl happens at higher strain levels as a result of successive bending and unbending when the steel goes over the die radius or any drawbeads. AHSS show greater stress-strain curves than HSS with the same yield stress and therefore greater springback for both angular change and sidewall curl distortions.
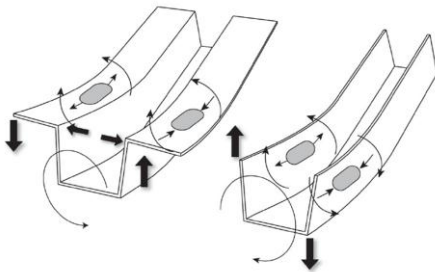
Figure 1: Channels and sidewall residual stresses [1]

A reliable forming process design can only be achieved with accurate prediction of part deformations early in the die-design phase. Although complex material models are currently developed and implemented in finite element packages, it has been observed that the FE predictions might not be satisfactory and estimated shapes for some industrial parts made of AHSS can be notably erroneous [2].

It is well known that FE analyses of sheet metal forming processes should be performed in two steps: an explicit incremental method applied to simulate the forming of the part, followed by an implicit FE approach with the forming geometry and stress distribution as the baseline input for springback analysis. It has been shown that

the material model, element formulation, contact algorithm and friction are important factors that affect the accuracy of springback simulations. The isotropic hardening plasticity models clearly do not account for specific behaviours of AHSS during cyclic deformations like Bauschinger effect, rapid change of material work hardening, early re-yielding or permanent softening. Besides, the isotropic hardening plasticity models usually produce an overrated cyclic hardening behaviour under a reverse loading. As a result, kinematic hardening models in conjunction with a backstress variable were introduced to describe the anisotropy of deformation such as the Bauschinger effect. In recent years, enhanced models for quantitative description of sheet metal deformations have been developed and implemented in commercial FE codes like LS-DYNA and ABAQUS.

However, two reasons have limited the usage of these advanced models in industrial applications: first is the increased number of material parameters necessary for the description of deformation, which requires more complex material testing and mathematical techniques to determine these parameters. The second issue is the cost associated with using these complex models compared to simpler material models. These issues were also addressed in a recent study for predicting springback of a 2D channel draw test for four steels grades including a dual phase and TRIP steel [3]. In this study, a comparison of LS-DYNA material models MAT36, MAT103 with a user-defined Yoshida-Uemori (YU) showed that the YU model is the most reliable and also the most expensive model to predict springback in high strength steels. In another report [4], MAT37 and MAT125 were used to describe the springback in a B-pillar made of DP780, and better results were reported for MAT125. In a later study [5], Zhu compared MAT37, MAT125 and a user-defined model for predicting experimental wall opening of hat stamped channels made of DP590 and DP780. Surprisingly, MAT125 demonstrated relatively poor performance but this was attributed to an incorrect implementation of the YU model. Ghaei et al. [6] used the YU model implemented in ABAQUS subroutines to simulate forming of a U-channel draw in presence of drawbeads and the subsequent springback stage. The results of this study showed good correspondence between the predicted and experimental springback cross-section profiles of DP600 channels using the YU model compared to the combined isotropic-nonlinear kinematic hardening model. Other investigations have also suggested that modification of YU model is needed to make it suitable for AHSS applications [7].

In the context of the present study, experimental results for a U-channel drawing of DP980 and TRIP780 steels are compared with simulated predictions using material models from the LS-DYNA material library [8]: MAT24, 36, 37, 125. The objective is to assess the ability of these models to accurately predict sidewall curl. The commercial FEA solver LS-DYNA971, R5.1.1 was used to perform the simulations on a Linux host. The material parameters for these models were identified in a series of laboratory tests and calibrated using LS-OPT [9].

U-channel Modeling

A channel forming process - previously presented as Benchmark #3 in Numisheet 2005 conference - was used here in order to assess the capability of various material models to predict sidewall curl. The draw die was installed at a local stamping plant (NARMCO) in a Williams/White hydraulic 600-ton press (Fig. 2), for the analysis of different grades of advanced high strength steel sheets, TRIP780 and DP980. The draw die was constructed in such a way that the material in the channel sidewalls was formed over a drawbead and a die entry radius, thus work hardening the sheet by cyclic bending and unbending in the drawbead and over the die radius. Blanks were sheared to a width of 254 mm so that the channel sidewalls would be stretched in plane strain.

A schematic of the draw die in its open position is shown in Fig. 3. This tool consists of an upper moving die section, a floating binder mounted on six cylinders pressurized by Nitrogen and a fixed lower punch. The upper die is equipped with changeable inserts on each side that provide different die entry radii as well as different inboard and outboard drawbead configurations. In this project no outboard drawbeads were used and flat blocks were inserted in their locations. A data acquisition application developed in LabView was used to capture various experimental

Figure 2: U-Channel draw die [10]

data during the drawing operation such as the force and displacement of the punch and binder.
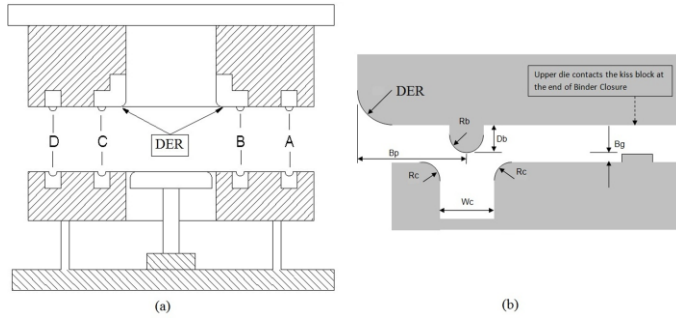
Figure 3: (a) schematic view of the die with changeable inserts with various die entry radius and drawbeads; (b) dimensional parameters of die drawbead block and kiss block on the binder shown in open position [10]

In this work, channels were formed with round, 4-mm diameter drawbeads set to a shallow bead depth. A constant kiss gap of around 30% more than material thickness was maintained during the forming stage in order to minimize the effects of friction. Also the blanks were uniformly sprayed with drawing oil before forming channels.

The FE model of the channel draw (Fig. 4) was created using quadrilateral 3D shell elements, with tools modeled as rigid materials. An initial size of 3 mm was used for the blank mesh with 4 levels of mesh adaptivity refinements and an adaptive error tolerance of 5 degrees relative to the surrounding elements. Since the springback analysis follows the forming simulation, fully integrated shell element formulation (type 16) was used both for the forming and sprinback models with 9 integration points through the thickness. Due to symmetry, only a quarter of the system was modeled in LS-DYNA. Three contact interfaces with algorithm type "Forming one way surface to surface" were defined between the blank and tools interfaces with a static friction coefficient equal to 0.125. Since only a limited area of the blank was in contact with the die radius and drawbeads, and the contact area did not change significantly during the drawing stage, it was reasonable to assume a steady-state forming process.

For the purpose of this study, the blank was modeled with four different models from LS-DYNA material library:

- MAT24 : Piecewise Linear Plasticity
- MAT36: 3-Parameter Barlat
- MAT37: Transversely Anisotropic Elastic Plastic
- MAT125: Kinematic Hardening Transversely Anisotropic (Yoshida-Uemori model)

The model parameters for TRIP780 and DP980 materials were identified from uniaxial tensile and cyclic tests that are described elsewhere [9]. Specific material model parameters used in this study are summarized in Table 1.
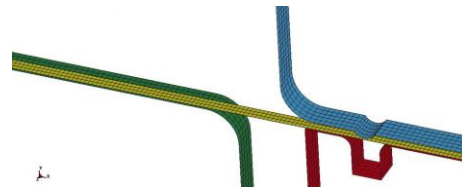
Figure 4: Finite element model of the channel draw forming in LS-DYNA

Parameter		TRIP780	DP980
Blank thickness, mm		1.2	1.5
Density, g/cm^3		7.85	7.85
Elastic modulus, GPa		207	207
Poisson ratio		0.28	0.28
Yield strength, MPa		450	652
r-value, average		0.89	0.78
m exponent for Barlat's yield surface		6	6
Coefficients for variation of elasticity modulus	saturated unloading modulus, E_a (GPa)	132.7	157.8
	rate of decrease, ζ	46.1	57.5
Yoshida parameters	B, (MPa)	448.9	775.5
	C	342.2	239.7
	R_{sat}, (MPa)	869.6	109.8
	K	5.25	68.73
	B, (MPa)	371.3	257.2
	h	0.295	0.821

Table 1. Material parameters for LS-DYNA models: MAT24, 36, 37 and 125

The predicted punch force computed in the FE analysis of the forming stage were compared with the forces experimentally measured with load cells that were placed underneath the fixed punch. As shown in Fig. 5a and b, the punch force is overestimated by material models MAT24, 36 and 37 (with isotropic hardening [IH]) and underestimated by MAT125 model for both TRIP780 and DP980 when drawbeads are used. Overestimation of IH models could be attributed to the failure of such hardening to capture the Bauschinger effect, and therefore the material response is over-predicted during cyclic loading.

(a)   (b)
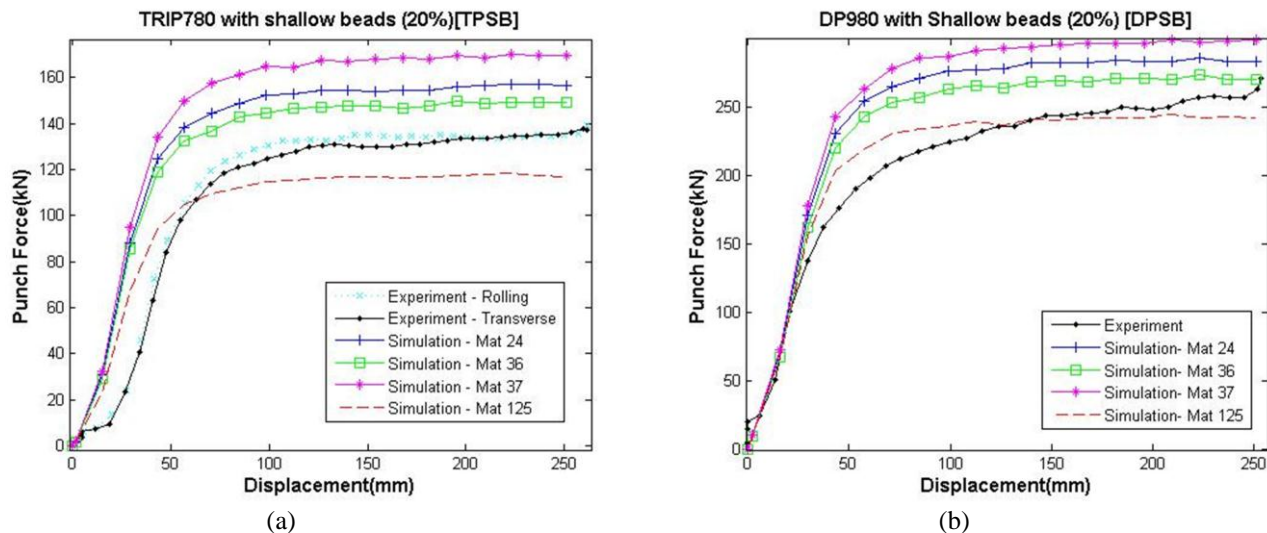
Figure 5: Comparison of predicted and experimental punch force results with various material models for channels made of: (a) TRIP780, (b) DP980.

The final geometry of the U-channels after springback is an important measure for comparison between different models. The error between simulated and experimental channel profiles was quantified by computing the area under the curves of both profiles drawn on a 2D diagram, as shown in Fig. 6. As the experimental and simulated profiles might not necessarily have one-to-one analogy, an interpolated profile was constructed on each of the curves on their common range for more accurate comparison using a Matlab code.

The difference between each point C on the experimental curve can be obtained with respect to its counterpart point C' on the simulated curve. Simulated curves were constructed from nodal coordinates read from the final geometry of the channels after springback. Therefore, the error at each point was calculated as δ_C from difference in both X- and Y-directions:

$$\delta_C = \sqrt{(X_C - X_{C'})^2 + (Y_C - Y_{C'})^2}$$

The sum of errors over the common portion of the sidewall curves was calculated by line integral method. By dividing the sum of errors by the area under the experimental curve from point A to B, the normalized error between corresponding experimental and simulated sidewall profiles can be calculated:

Figure 6: Schematic illustration of sidewall comparison between simulated and experimental curves

$$Sidewall\ error\ (\%) = \frac{\text{Area between curves, integral of } \delta_C}{\text{Area under experimental curve from A to B}}$$

Results of channel sidewall profile comparison for various configurations as well as the relative error of the sidewall curl are shown in Figs. 7 and 8 for TRIP780 and DP980, respectively.

(a)   (b)
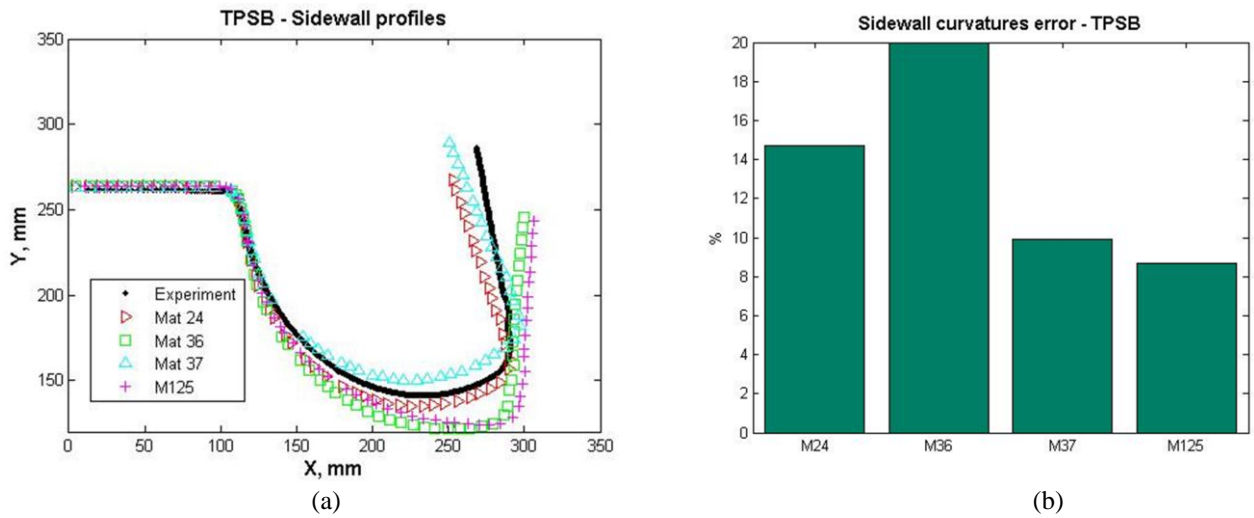
Figure 7: Comparison of simulated and experimental sidewall profiles for TRIP780 channels with shallow beads: (a) different material models, (b) sidewall error

(a)   (b)
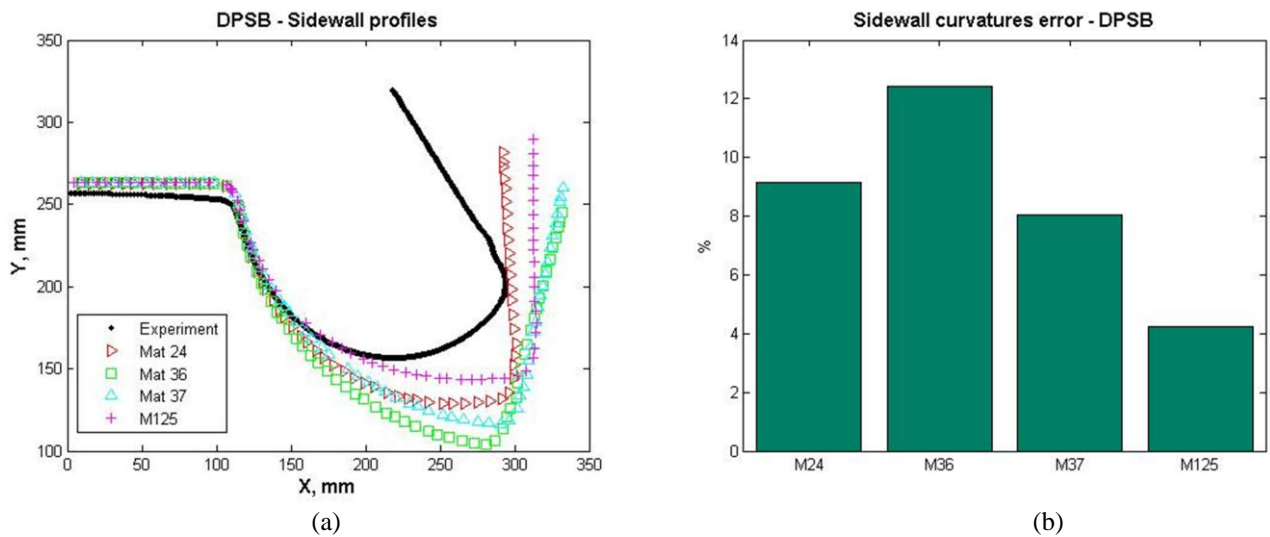
Figure 8: Comparison of simulated and experimental sidewall profiles for DP980 channels with shallow beads: (a) different material models, (b) sidewall error

It can be seen that MAT125 produced the minimum amount of error in terms of the sidewall curl error with respect to the other material models. However, the predicted channel profiles of DP980 showed greater error on the flange tip with respect to the experimental results compared with TRIP780 channels.

The predicted FLD curves for forming process of channels are compared in Fig. 9. a & b for TRIP780 and DP980, respectively. It can be seen that the plane-strain condition prevails in both predictions. The predicted values of the major strain in the central region of the channel sidewall were also comparable with the experimental circle grid measurements in this region, 4% for TRIP780 and 3% for DP980 channels.

(a)   (b)
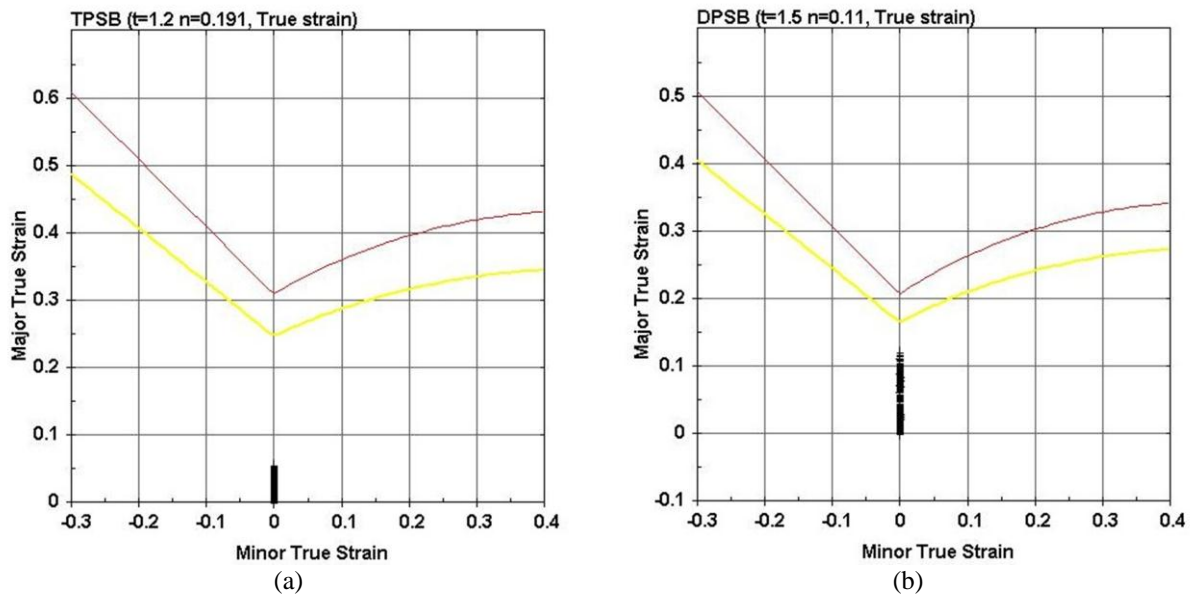
Figure 9: FLD with strain data predicted for: a) TRIP780 and b)DP980 channels

Industrial applications

The forming and springback of two industrial auto body parts known as B-pillar and a doubler inner part, both made of DP980 steel sheet with a thickness of 1.5 mm were simulated with LS-DYNA. Based on the findings from the channel draw simulations in previous section, material models MAT37 and MAT125 were used in the FE modeling of these parts to identify which model produces the most accurate results. Shell elements with 9 integration points through the thickness and fully integrated element formulation (type 16) were used for the blank. Adaptive meshing and other control parameters were assigned similar to the channel forming simulations. The deformed parts after the forming stage were submitted to an implicit springback solution by fixing appropriate nodes to eliminate rigid body motions.

The B-pillar part was modeled in a single crash forming operation as shown in Fig. 10, while the simulation of the doubler inner part included two forming stages as shown in Fig. 11 a. & b.
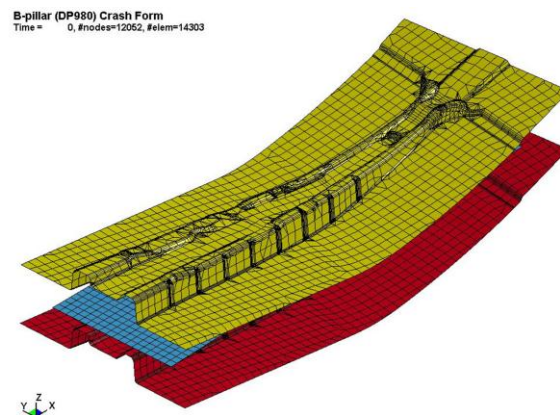
Figure 10: FE modeling of a B-pillar forming operation

Doubler Inner - Forming 1
Time =   0, #nodes=3918, #elem=4079

Doubler Inner - Forming 2
Time =   0, #nodes=20642, #elem=19770

(a)   (b)
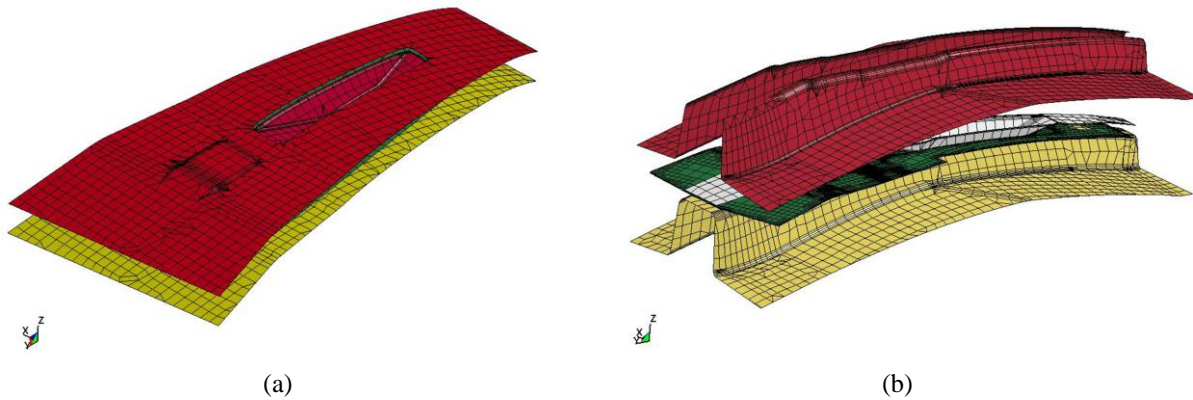
Figure 11: FE model of a B-pillar doubler inner part: a) first forming, b) second forming

The results of final springback simulations with MAT37 for both parts are shown in Figs. 12 and 13. The contour of the parts after the springback was overlaid on the featured geometries at the end of the forming stages.

B-pillar springback
Time =   0.004
Contours of Effective Plastic Strain
max IP. value
 min=0, at elem# 38840
 max=0.434475, at elem# 70201

Fringe Levels

4.345e-01
3.983e-01
3.621e-01
3.259e-01
2.896e-01
2.534e-01
2.172e-01
1.810e-01
1.448e-01
1.086e-01
7.241e-02
3.621e-02
0.000e+00
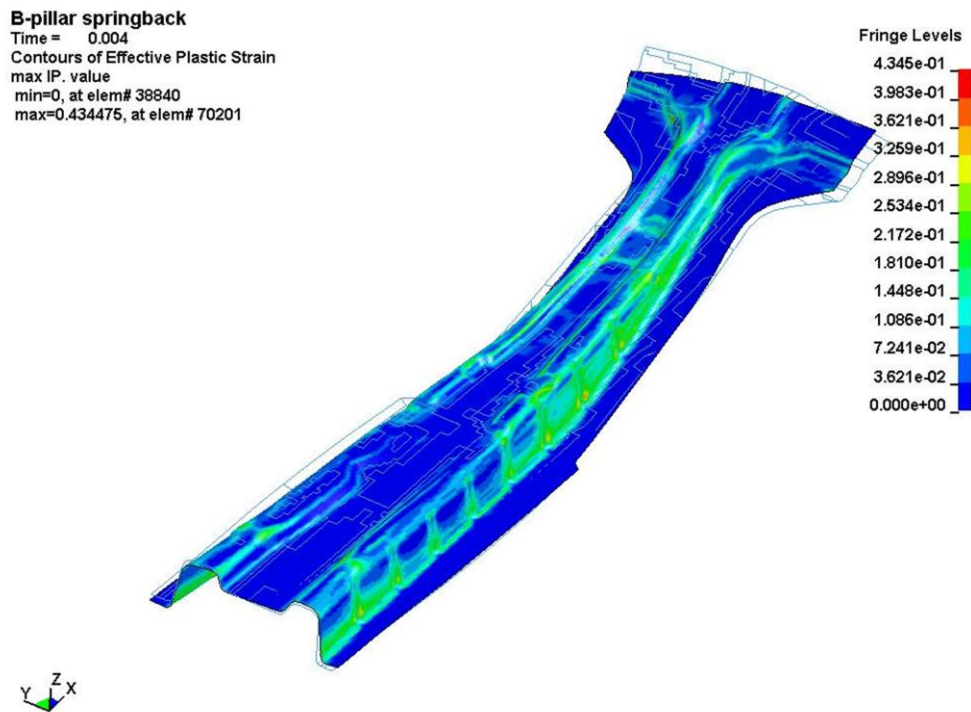
Figure 12: Comparison of fully formed (lines) and sprungback B-pillar with material model 37

Doubler Inner - springback
Time =   0.004
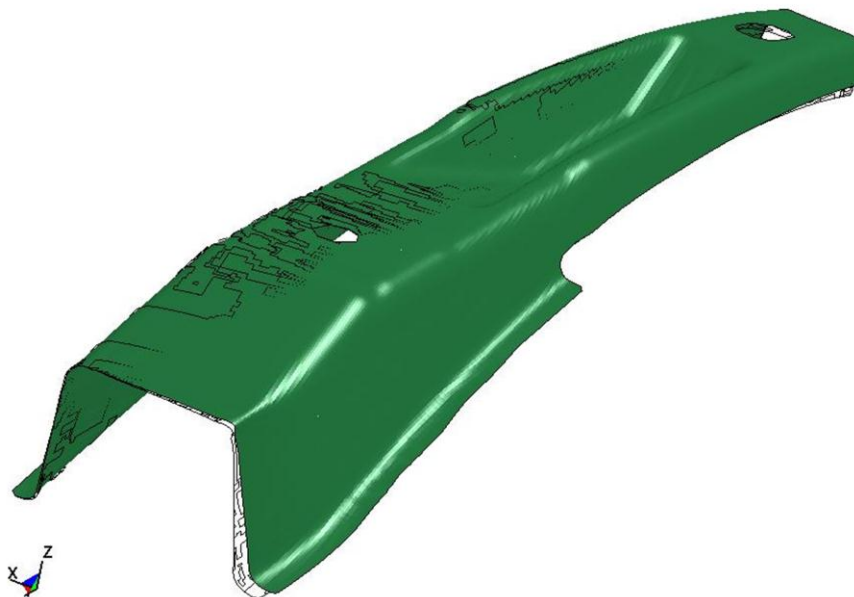
Figure 13: Comparison of fully formed (lines) and sprungback Doubler inner with material model 37

Simulations with material model MAT125 did not converge to a solution for either of the industrial parts. The reason may be an incorrect implementation of the model MAT125 in LS-DYNA considering that the identical input file was used with model MAT37. Although material input parameters for the YU model from other studies and different steel grades ([6], [7] and [11]) were also tested with the model 125, it was observed that the non-convergence of the plasticity model MAT125 for complex geometries is not related to numerical values alone.

Conclusions

In this study, drawing and springback of a plane-strain channel section made from advanced high strength steel, DP980 and TRIP780 were simulated with LS-DYNA and the sidewall curl was predicted with four different material models: MAT24, 36, 37 and 125. Two industrial parts made of DP980 were also studied using the findings from the channel draw. The following major conclusions were reached:

1- Material model MAT125 predicted the most accurate sidewall curl results for simple geometries like the plane-strain channel draw process compared to models MAT24, 36 and 37 from LS-DYNA material library.

2- Experimental and numerical simulations similarly confirmed that channels made of DP980 exhibit more sidewall curl than those made of TRIP780.

3- For two more complex geometries modeled with shell elements, material model MAT125 did not converge to a final solution of forming and springback while model MAT37 predicted more accurate springback results than MAT24 and MAT36.

4- Further work is required for robust implementation of the YU model either as a user material model or through improving model MAT125 from the LS-DYNA material library.

Acknowledgements

References

[1] "Advanced high strength steel application guidelines", Version 4.1. World Auto Steel, June, 2009 www.worldautosteel.org

[2] Du C., Chen X. M., Lim T., Chang T., Xiao P., and Liu S. D., "Correlation of FEA prediction and experiments on dual-phase steel automotive rails", AIP Conference Proceedings, 908(1), 2007, pp. 943-948, doi:http://dx.doi.org/10.1063/1.2740932

[3] Aydin M.S., Kessler L., Gerlach J., "Springback simulation with complex hardening material models", Proceedings of LS-DYNA Conference, Bamberg, Germany, 2008.

[4] Du C., Chrysler Group, LLC, "Advanced High Strength Steel Stamping – ASP050", Annual Progress Reports – Lightweighting Material, Nov. 2010, http://www1.eere.energy.gov

[5] Zhu H., Sriram S., Yan B., and Duroux P., "Advanced material characterizations and constitutive modeling for AHSS springback predictions," SAE International Journal of Materials Manufacturing, 3(1):691-701, 2010, doi:10.4271/2010-01-0980

[6] Ghaei A., Green D. E., Taherizadeh A., "Semi-implicit numerical integration of Yoshida-Uemori two-surface plasticity model", International Journal of Mechanical Sciences, 52: 531-540, 2010.

[7] Shi M.F., Zhu X., Xia C., Stoughton T., "Determination of nonlinear isotropic/kinematic hardening constitutive parameters for AHSS using tension and compression tests", Proceedings of NUMISHEET Conference, Switzerland, pp: 264-270, 2008.

[8] Livermore Software Technology Corporation (LSTC), "LS-DYNA keyword user's manual", Vol. I. version 971, 2007.

[9] Aryanpour A., Green D. E., Van Tyne C. J., Rothleutner L., Rodzik M. "Characterization of advanced high strength steel sheets in view of numerical prediction of sidewall curl", submitted to the Journal of Materials Processing Technology, 2012.

[10] Aryanpour A., "Experimental and Numerical Analysis of Sidewall Curl in Advanced High Strength Steels", 2011, Master's thesis, University of Windsor, http://knowledge.library.utoronto.ca/apache/etheses/windsor/aryanpo_ethesis.pdf

[11] Ma N., Umezu Y., Watanabe Y. and Ogawa T., "Springback prediction by Yoshida-Uemori model and compression of tool surface using JSTAMP", Proceedings of NUMISHEET Conference, Switzerland, pp: 473-478, 2008.